Desalination 344 (2014) 431–445

Contents lists available at ScienceDirect

Desalination

journal homepage: www.elsevier.com/locate/desal

Minimizing the total cost of multi effect evaporation systems for seawater desalination

Paula Druetta, Pio Aguirre, Sergio Mussati *

INGAR, Instituto de Desarrollo y Diseño (CONICET-UTN), Avellaneda 3657, S3002GJC Santa Fé, Argentina

HIGHLIGHTS

- An optimization mathematical model of MEE is presented.
- Investment and operating costs are minimized for a nominal water demand.
- A sensitivity analysis of the main parameters and variables is presented.
- Detailed solutions and a complete discussion of the results are presented.

ARTICLE INFO

Article history:
Received 3 July 2013
Received in revised form 19 March 2014
Accepted 6 April 2014
Available online 3 May 2014

Keywords:
Multi-effect evaporation systems
Optimization
Total annualized cost
Non-linear programming (NLP)

ABSTRACT

A mathematical model developed recently by the authors is extended into a non linear mathematical programming problem to determine the nominal optimal sizing of equipment (heat transfer area) and optimal operation conditions that satisfy a fixed nominal production of fresh water at minimum total annual cost. Relative marginal values computed from the optimized results and a global sensitivity analysis are then used to rank the process parameters according to their influences on the total cost. Once the nominal design and operating conditions are determined, a new optimization problem is stated: Is it possible to increase (using the nominal optimal design) the water production over the nominal capacity of production? Thus, the new optimization problem consists of the maximization of the distillate production. Optimization results for both design problems are presented and discussed in detail. One of the obtained results reveals that the increase of the distillate production in 20% over the nominal capacity (200 kg/s), leads to increases in the total operating cost from 10.8 to 11.4 million US$/yr while the seawater flow rate and the steam temperature increase about 23 and 5%, respectively.

1. Introduction

Despite the significant progress on the desalination processes made since the 1960s to overcome the problem of fresh water supply [1], technological and research efforts are still required to improve the system's efficiency and to reduce the water production cost. The major challenge is to reduce the energy cost by improving the steam economy or performance ratio PR (kg of fresh water produced by kg of steam used) [2–4]. For the MEE system, there exist strong trade-offs between the steam used in the first effect as heating utility, the total heat transfer area for evaporation and pre-heating and production level. For a desired production of distillate, the reduction of the steam consumption increases the required total heat transfer area and vice versa. Several methodologies based on energy and/or exergy analysis have been applied to study the performance of MEE systems [5–7].

Several papers have been published over the last years, dealing with the thermo-economic analysis of different MEE systems. Instead of simultaneous and rigorous optimization methods, most of the authors applied parametric optimization and used several simulation software to study the influence of the operation conditions and the size of the evaporation effects on the performance of the MEE unit [8–10].

In contrast to these articles, the main contribution of this paper is that the operating conditions and size of each effect are optimized simultaneously instead of a parametric way. In addition, local and global sensitivity analyses for all model parameters, which are useful for both practical and mathematical modeling point of views, are also presented.

The application of the mathematical programming approach for the optimal design of desalination processes is receiving a renovated interest due to the fact that the performance of solvers handling non-linear constraints for simultaneous optimization was largely improved.

Recently, Druetta el at. [11] successfully applied the mathematical programming approach to optimize the MEE system from an efficiency

* Corresponding author at: Avellaneda 3657, S3002GJC Santa Fé, Argentina. Tel.: +54 342 453 5568, +54 342 4534451; fax: +54 342 455 3439.
E-mail addresses: pauladruetta@santafe-conicet.gov.ar (P. Druetta), paguir@santafe-conicet.gov.ar (P. Aguirre), mussati@santafe-conicet.gov.ar (S. Mussati).

http://dx.doi.org/10.1016/j.desal.2014.04.007
0011-9164/

point of view and to study different arrangement configurations. In this paper, the model presented in [11] is properly extended in order to include a complete and detailed cost model to determine the optimal size of equipment and optimal operation conditions that satisfy a given nominal production of fresh water at minimum total annual cost. After that, a second optimization problem is solved in order to identify the operating conditions that should be modified in order to increase the distillate production over the nominal capacity production. The results obtained for both optimization problems are discussed and compared in detail. In addition, for both optimization problems, local and global sensitivity analyses are also performed in order to evaluate the relative importance of each one of the model parameters. Qualitative and quantitative results obtained from the analyses will provide valuable insights for the design of new MEE plants or, if the case, for the identification of alternative operating modes in existing plants with the main aim to improve the process efficiency. To the knowledge of the authors, no articles addressing local and global sensitivity analyses of all process parameters have been published.

The parameters to be analyzed are defined in several sets, as follows.

a) Sea water conditions. The sea water salinity and temperature vary with the plant location and the season of the year. From a thermal integration point of view a sensitivity analysis on these parameters may be valuable because it may identify several hybrid desalination systems. In other words, it may indicate the convenience (or not) to integrate the seawater incoming with other processes.
b) Physical–chemical properties and design specification. Usually, most of the hypotheses used to derive simplified mathematical models consider that several physical–chemical properties do not significantly vary with temperature, composition and/or pressure and therefore they are considered as model parameters (fixed and known values). Similarly, a given value is usually assumed for overall heat transfer coefficients to compute the heat transfer areas. However, in some cases, it may not be appropriate. A sensitivity analysis on these parameters will determine the correctness of the hypothesis. Thus, it will provide useful insights about the convenience of use of correlations instead of a fixed and known value.
c) Operating conditions. A sensitivity analysis will allow us to identify the operating conditions that may improve the process efficiency or may minimize the total cost. For instance, it is important to know, for an existing MEE unit, the operating variables that must be modified to increase the distillate production.
d) Specific costs. The specific costs used to compute investment and operating costs may vary significantly with place and time. Therefore, it is also essential to know how they affect the total annual cost.

The paper is outlined as follows. Section 2 briefly describes the MEE process and presents the problem formulation. Section 3 summarizes the assumptions and describes the mathematical model. Section 4 discusses the simulated and optimized results obtained from the model. Finally, Section 5 summarizes the conclusions of the paper.

2. Process description

Fig. 1 shows a schematic diagram of the MEE forward feed scheme which will be studied in this paper. As shown, the brine stream (B) and the distillate (D) flow in the same direction but opposite to the feed stream (F). The first effect is characterized by the least salinity and the highest temperature. The feed stream (F) is heated in preheaters by the condensation of vapor produced in each one of the effects. Then, F enters into the first evaporation effect and a part of the produced vapor (V^p_1) is used for pre-heating in the pre-heater 1 and the remaining vapor (V_2) is used for evaporation in the Effect 2. Then the condensate coming from the preheater 1 and the evaporation effect 2 are flashed into the flashing box 2. The process is repeated along the remaining effects.

There exist several trade-offs among the total heat transfer area, heating utility demand (steam), mass flow rates, production level and electric power consumption. Then, the main objective of this paper is to minimize the total annual cost of the MEE unit (investment and operating costs) but considering all the trade-offs simultaneously.

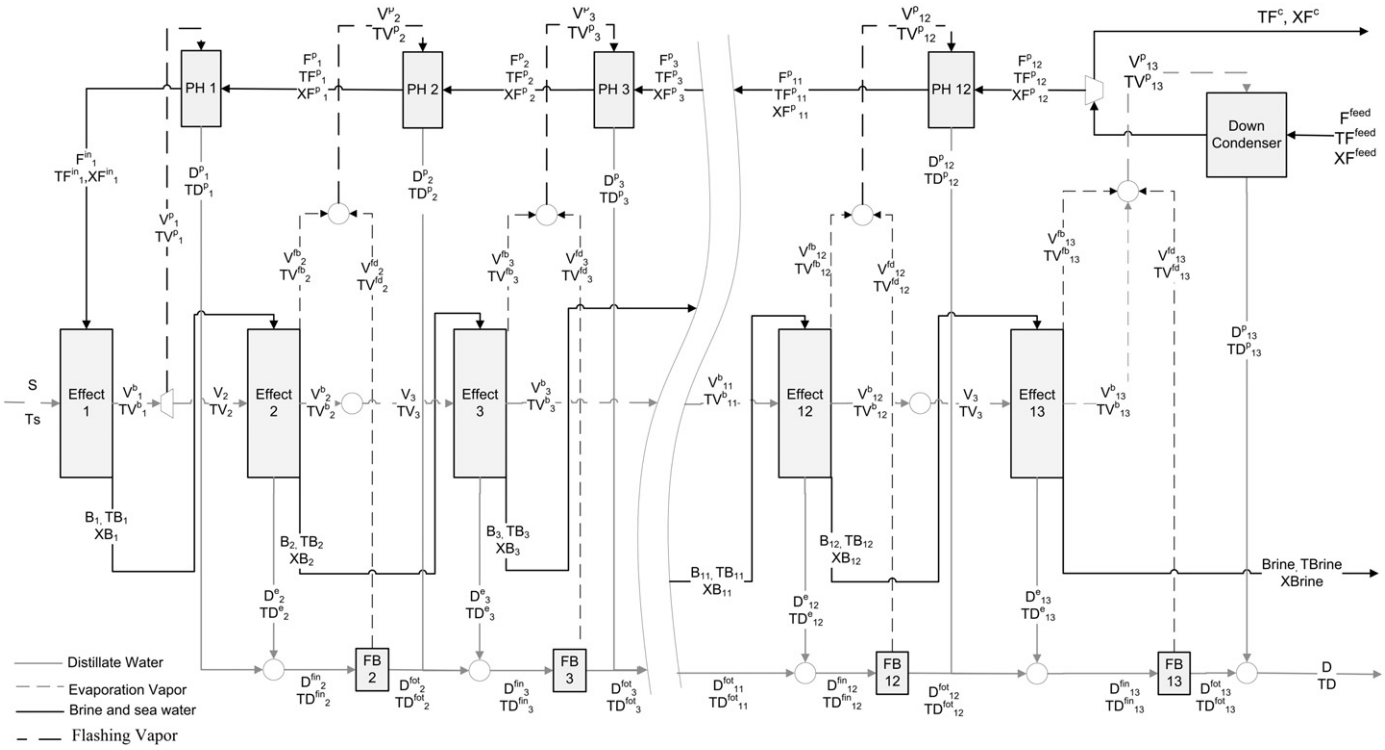

Fig. 1. Conventional multi-effect evaporation (MEE) process (forward feed configuration).

Next, the problem statement, assumptions and mathematical model are presented.

Given the fresh water demand to be satisfied and the seawater specifications (temperature and salinity), the goal is to determine the optimal operating conditions (flow-rate and temperature of each stream) and the size of each piece of equipments (heat transfer area required by the evaporation effects and pre-heaters) in order to minimize the total annual cost (TAC) which includes investment and operating costs.

Mathematically, the optimization problem can be expressed as follows.

To minimize (or maximize) z(x)subject to:

$$h_s(x) = 0 \quad \forall s$$
$$g_t(x) \leq 0 \quad \forall t$$

where x is the vector of model variables, z (total annual cost, distillated water production, etc.) is the objective function to be optimized [min. total annual cost or max. distillate production], $h_s(x)$ refers to equality constraints (mass and energy balances, correlations for computing physical–chemical properties, pressure drops, design equations, cost equations) and $g_t(x)$ refers to inequality constraints, which are usually proposed to avoid temperature crosses and impose lower and upper bounds in some critical operating variables. For instance, in order to consider environmental aspects, upper bounds on the rejected brine temperature and salinity are included as follows: $TB_N \leq TB^{up}$ and $XB_N \leq XB^{up}$. Thus, T^{up} and XB^{up} will refer to the upper bounds of TB_N and XB_N respectively.

3. Assumptions and mathematical model

3.1. Assumptions

In order to derive a simple and accurate prediction mathematical model to study the steady-state MEE process, the following assumptions are considered.

- A constant and known value is assumed for: the boiling point elevation (BPE), the specific heat capacity at constant pressure of brine (CP^b), the latent heat (λ), the average density (ρ) and viscosity (ν), pump output pressure, equipment efficiencies.
- A different but a constant and known value is assumed for each overall heat transfer coefficient in the down-condenser, pre-heaters and evaporators.
- The heat transfer area distributions along the evaporation effects and pre-heaters (UHTA) are assumed to be uniform.
- The total flashing vapor obtained in the evaporators and in the flashing boxes is only used to preheat the feed.
- The seawater stream is chemically treated after it leaves the down condenser.
- The product is considered to be free of salts.
- The sea water specifications (salinity and temperature), the heating steam temperature, the specific costs related to investment and operating costs, the lifetime of the plant and the annual interest rate are assumed to be model parameters (known and fixed values).
- Environmental aspects are included. Precisely, the temperature and salinity of the rejected brine are controlled by including upper bounds.
- As a first approximation to derive a simplified mathematical model the dimensions of each effect (length, width and height) are not included in the model. Therefore, the pressure drop during the vapor condensation process and the pressure drop in the demister are not considered. In addition, the electrolyte thermodynamics to predict the CO_2 release rates is also not included. Therefore, the presence of non-condensable gases on the heat transfer coefficients in the evaporators, pre-heaters and down-condenser are not considered.

3.2. Mathematical model

As mentioned earlier, the steady-state mathematical model of the MEE forward feed schema including the configuration of streams shown in Fig. 1 was already developed and successfully verified in Druetta et al. [11].

Basically, the steady-state mathematical model of the MEE forward feed schema including the configuration of streams shown in Fig. 1 based on the mass and energy balances around each one of the process-units (mixers, splitters, evaporation effects, distillate flashing chambers and pre-heaters). This model of the MEE desalination system was already developed and successfully verified in Druetta et al. [11]. Thus, in this section, only the new constraints related to the cost model are presented.

3.2.1. Cost model

The specific total annual cost (sTAC) is computed as follows:

$$sTAC = \frac{TAC}{D\ THY\ 3600} \quad (1)$$

Table 1
Numerical values of parameters.

Parameters		Value
Sea water		
TF^{feed}	(°C)	24.00
XF^{feed}	(ppm)	43,000.00
Physical–chemical properties		
CP^b	(kJ/kg °C)	4.00
BPE	(°C)	1.50
λ	(kJ/kg)	2375.00
ρ^b	(kg/m^3)	1060.00
ρ^p	(kg/m^3)	1000.00
ν^b	(kg/m s)	0.001
Design specifications		
N		13
D	(kg/s)	200.00
T^{up}	(°C)	45.00
XB^{up}	(ppm)	120,000.00
U^e	(kW/(m^2 °C))	3.00
U^p	(kW/(m^2 °C))	2.50
U^c	(kW/(m^2 °C))	2.00
TS	(°C)	80.00
ΔP^{in}	(bar)	5.00
Dca	(m)	0.02
Dci	(m)	0.016
THY	(h/yr)	8000.00
RHC		0.25
RHin		0.30
RHout		0.60
RHben		0.30
η		0.75
Specific costs		
K^{MEE}	($/m^2)	3644.00
K^C	($/m^2)	500.00
Cpow	($/kWh)	0.09
Cswip	($/(m^3/d))	50.00
Cch	($/m^3)	0.024
Cstm	($/kg)	0.00415
Clab	($/m^3)	0.05
Time	(yr)	20.00
$Cmat^{MEE}$		1.40
$Scal^{MEE}$		0.54
$Cmat^C$		2.80
$Scal^C$		0.80
Ir		0.06

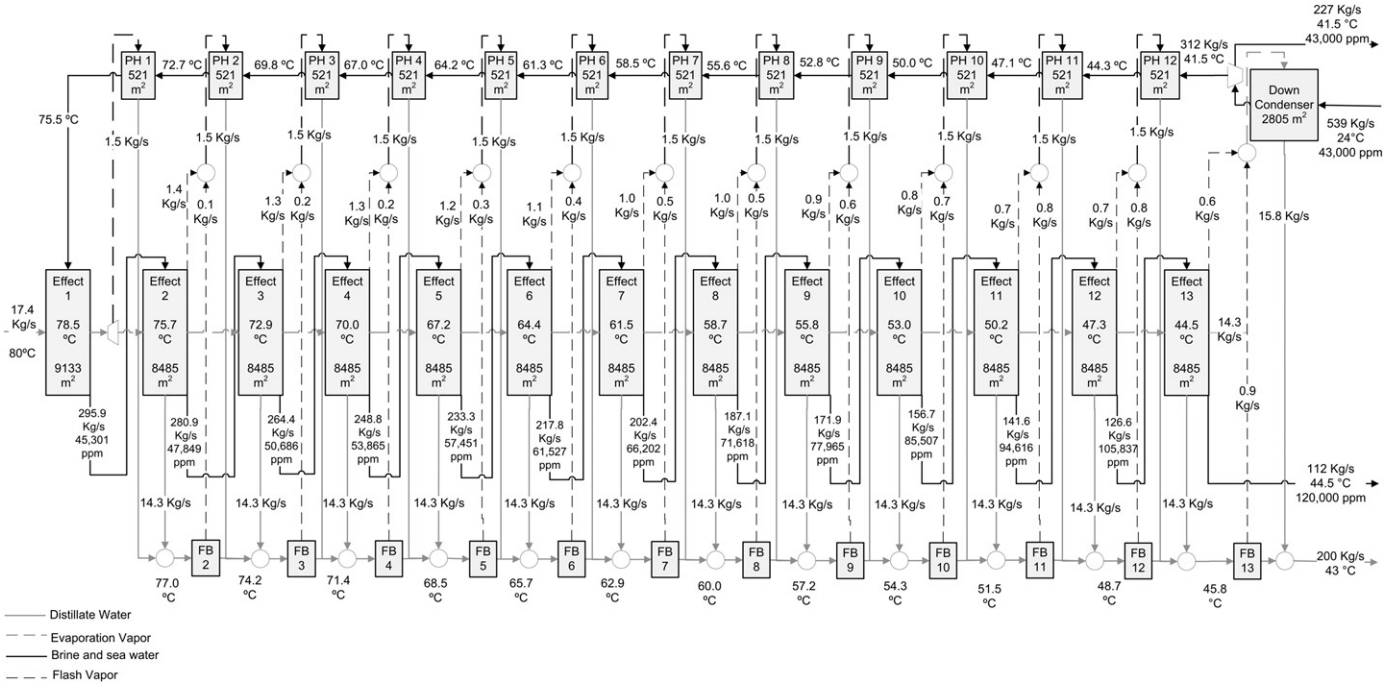

Fig. 2. Optimal solution for a fresh water production of 200 kg/s.

where, the total annualized cost (TAC) is given by Eq. (2) and takes into account the total annualized investment (TCC) and the operating cost (AOC).

$$TAC = (AOC + CRF \times TCC) \tag{2}$$

where CRF refers to the capital recovery factor. The total capital cost (TCC) includes the direct and indirect capital costs (CCDir and CCIndr respectively) as indicated in Eq. (3) [11,12].

$$TCC = CCDir + CCIndr \tag{3}$$

CCDir is computed in terms of the total equipment cost (CCeq) and civil work capital cost (CCcw) and is used to compute the indirect cost CCIndr, as indicated below.

$$CCDir = CCeq + CCcw \tag{4}$$

$$CCIndr = 0.25\ CCDir \tag{5}$$

Table 2
Optimal values for other important design and operational variables of the system.

Variables		Value
$LMTD^c$	(°C)	6.70
$LMTD_1$	(°C)	2.68
$LMTD_p$	(°C)	2.72
ΔT		1.34
A^b_1	(m^2)	4.71×10^2
A^e_1	(m^2)	8.7×10^3
sA	(m^2/(kg/s of D))	600.03
PR	(ton of D/(ton/s of S))	11.30
CR	(ton/s of D/(ton/s of F))	0.64
sWc	(ton/s of F^c/(ton/s of D))	1.13

Then, the following equations are used to compute CCcw and CCeq:

$$CCcw = 0.15\ CCeq \tag{6}$$

$$CCeq = CCswip + CCMEE + CCCond \tag{7}$$

where CCswip, CCMEE and CCCond refer, respectively, to the investment related to the seawater intake and pre-treatment, MEE unit and down condenser which are computed from Eqs. (8) to (11). Each one of the cost-items of the total equipment capital costs were computed as follows [14].

$$CCswip = KCswip\ F^{MEE} \tag{8}$$

$$CCMEE = Carea^{MEE}\left(A^{MEE}\right)^{scal^{MEE}} \tag{9}$$

Table 3
Optimal values for the main economic variables.

	Variables	Values
sTAC	(US$/$m^3$)	0.63
TAC	(million US$/yr)	3.60
TCC	(million US$)	16.60
	CCIndr	3.31
	CCDir	13.20
	CCcw	1.73
	CCeq	11.50
	CCMEE	8.53
	CCswip	2.19
	CCcond	0.80
AOC	(million US$/yr)	2.16
	OCst	1.04
	OCpow	0.38
	OClab	0.29
	OCch	0.20
	OCman	0.17
	OCins	0.08

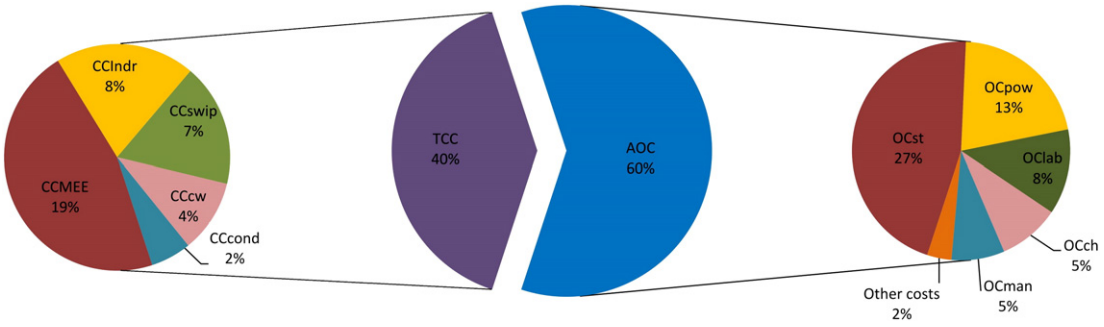

Fig. 3. Relative influence of each one of the system costs.

where:

$$A^{MEE} = \sum_{j=1}^{N}\left(A_j^e\right) + A_1^b \tag{10}$$

$$CCcond = Carea^c\ (A^c)^{scal^c}. \tag{11}$$

The cost of the MEE unit (CCMEE) includes the heat transfer area related to the evaporation effects and pre-heaters and the pumping system. For a more accurate calculation, CCcond is computed separately from the remaining heat transfer area.

Then, KCswip, $Carea^{MEE}$, $Carea^c$ are computed as follows. The corresponding numerical values used in each equation are listed in Section 5.

$$KCswip = \frac{Cswip\ 24\ 3600}{\rho^b} \tag{12}$$

$$Carea^{MEE} = Cmat^{MEE}\ K^{MEE} \tag{13}$$

$$Carea^c = Cmat^c\ K^c \tag{14}$$

Table 4
Local sensitivity analysis — Relative marginal values (RMV).

Parameters		Value	RMV
λ	(kJ/kg)	2375.00	0.35
K^{MEE}	($/m^2)	3644.00	0.35
Cstm	($/kg)	0.004	0.28
TF^{feed}	(°C)	24.00	0.25
TS	(°C)	80.00	−0.23
BPE	(°C)	1.50	0.22
U^e	(kW/m^2 °C)	3.00	−0.19
ρ_b	(kg/m^3)	1060.00	−0.17
D	(kg/s)	200.00	−0.16
η^{hpp}		0.75	−0.10
Cpow	($/kWh)	0.09	0.10
Cp^b	(kJ/kg °C)	4.00	−0.10
Cswip	($/(m^3/d))	50.00	0.09
Clab	($/m^3)	0.05	0.08
ρ_p	(kg/m^3)	1000.00	−0.08
ΔP^{in}	(atm)	4.95	0.07
Cch	($/m^3)	0.024	0.06
XF^{feed}	(ppm)	43,000.00	0.05
XB^{up}	(ppm)	120,000.00	−0.05
K^C	($/m^2)	500.00	0.03
Dca	(m)	0.02	−0.03
Dci	(m)	0.016	0.02
U^c	(kW/m^2 °C)	2.00	−0.02
U^p	(kW/m^2 °C)	2.50	0.02
ν^b	(kg/m s)	0.001	0.01

$$A^c = A_N^p \tag{15}$$

The numerical values used for Cswip, $Cmat^{MEE}$ and $Cmat^c$ are listed in Section 5.

The annual operating cost (AOC) is computed by Eq. (16)

$$AOC = OCCh + OCpow + OCst + OClab + OCman + OCins \tag{16}$$

Each cost-item included in Eq. (16) is computed as follows [13–16].

$$OCCh = KCch\ F_N \tag{17}$$

$$OCpow = KCpow\left(\left(1.01325\ \Delta P^{in} + \Delta P^c\right)F^{MEE} + \left(\Delta P^p + \Delta P^e\right)\ F_N^p\right) \tag{18}$$

$$OCst = KCStm\ S \tag{19}$$

$$OClab = KClab\ D \tag{20}$$

$$OCman = 0.001\ TCC \tag{21}$$

$$OCins = 0.005\ TCC \tag{22}$$

where:

$$KCch = \frac{Cch\ 3600\ THY}{\rho^b} \tag{23}$$

$$KCpow = \frac{100\ THY\ Cpow}{\rho^b \eta} \tag{24}$$

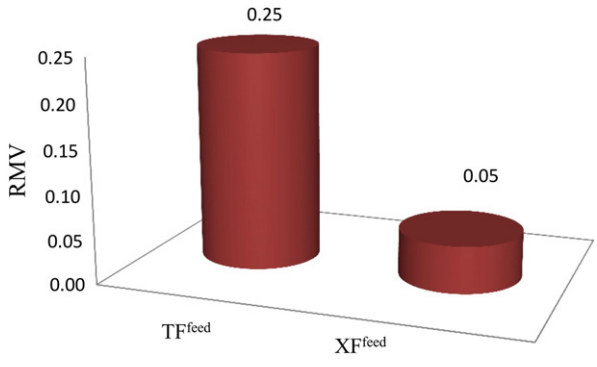

Fig. 4. Seawater parameters.

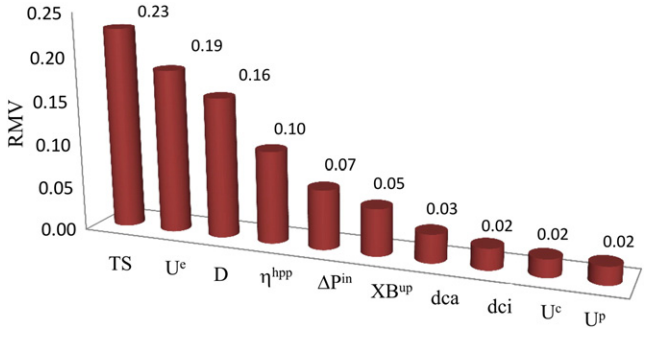

Fig. 5. Design and operational parameters.

$$KCStm = CStm\ \ 3600\ \frac{(TS\text{-}40)}{80}\ THY \tag{25}$$

$$KClab = \frac{Clab\ THY\ 3600}{\rho^{p}} \tag{26}$$

The pressure drop expressions are presented in Appendix A. The numerical values used for Cch, Cpow, CStm, Clab, THY, ρ^{p}, ρ^{b} and ΔP^{in} are listed in Section 5 (Table 1).

The set of equations described above [Eqs. (1) to (26)] plus the equations related to the mass and energy balances and that corresponding to compute the size of pieces of equipment presented in Druetta et al. [11] are used to solve the optimization problem stated in Section 2. The resulting optimization model involves 1078 constraints (equalities and inequalities) and 856 variables. It was implemented in GAMS (general algebraic modeling system) and CONOPT is used as a NLP local solver which is based on the Generalized Reduced Gradient (GRG). Global optimal solutions cannot be guaranteed due to the presence of non-convex constraints.

4. Discussion of results

4.1. Case Study 1: Minimization of the total annual cost (TAC)

This section discusses the results obtained for the optimization problem stated in Section 2. Then, local and global sensitivity analyses are also performed in order to evaluate the relative importance of each parameter on the total annual cost.

As mentioned in the introduction section the parameters are listed by sets according to their different characteristics (see Table 1). For a more reliable and precise reproducibility of the results and models verification, some values are presented with a different number of significant digits of precision.

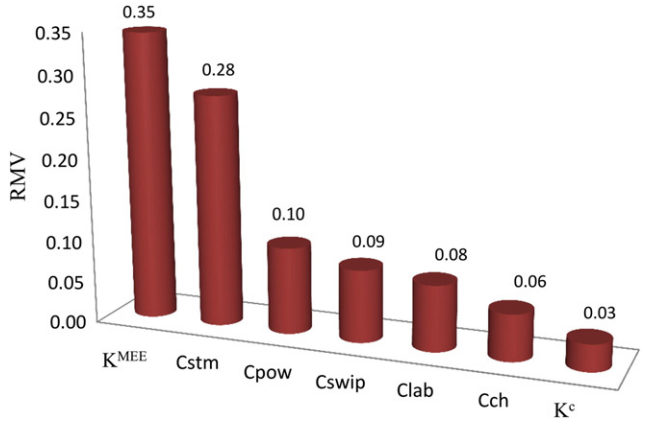

Fig. 6. Economical parameters.

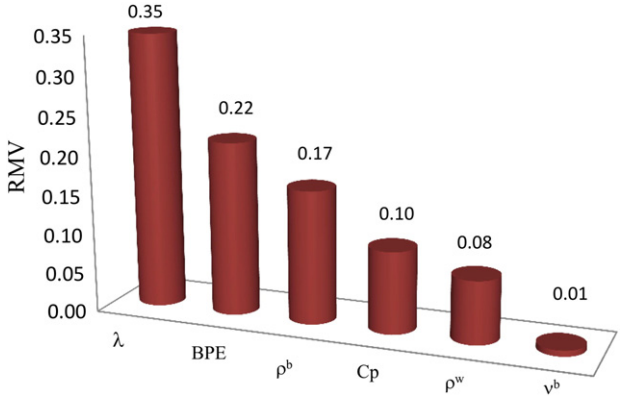

Fig. 7. Physical–chemical parameters.

Fig. 2 and Table 2 show the optimal values of the mass flow rate, temperature and composition of each stream and the heat transfer areas required in the evaporation effects and pre-heaters. Table 3 presents the total annual cost and how it is distributed in investment and operating costs.

The specific total annualized cost obtained from the model (0.63 US$/m^3) and the main efficiency parameters (S, PR, sWc, sA) are in good agreement with those reported in the literature [14, 17–20], despite that it is strongly dependent on several factors (specific costs used, source water, location, treatment process, and the size of the plant). The specific cost reported in the literature ranges from 0.50 US$/m^3 to 2.00 US$/m^3.

For a more detailed visualization of the results, Fig. 3 illustrates how the total annual cost is distributed in operating cost (AOC) and investment (TCC). The contributions of the operating cost and investment on the total cost for the entirely desalination system are 60.0 and 40.0%, respectively. Also, Fig. 3 shows that the costs of steam used as heating utility (OCst) and electricity consumed by pumps account for approximately 29 and 10% of the TAC, which represent 48 and 18% of the AOC, respectively; while the CCMEE contributes more than 20% of the TAC (51% of the TCC).

4.1.1. Sensitivity analysis of the model parameters on the total cost

In order to investigate the influence of each one of the model parameters (P_j) on the total annual cost, both local and global sensitivity analyses are performed. As mentioned earlier, these analyses are important and valuable because, in many situations, the system of equations depends on parameters which are not exactly known. Then it is interesting

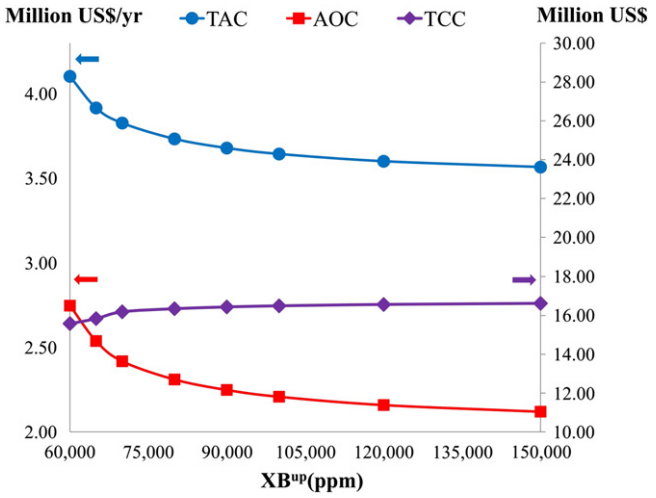

Fig. 8. TAC, AOC and TCC vs XB^{up}.

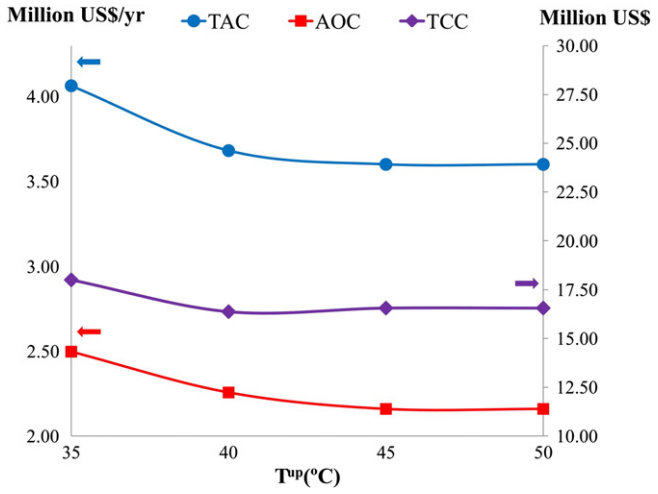

Fig. 9. TAC, AOC and TCC vs T^{up}.

to estimate the rate of change in the model outputs respect to changes in the model inputs. Such knowledge is important for (a) evaluating the applicability of the model, (b) determining parameters for which it is important to have more accurate values, (c) understanding which are the parameters that have a greater effect on the system cost and (d) understanding the behavior of the system being modeled. The choice of a sensitivity analysis method depends mainly on (a) the sensitivity measure employed, (b) the desired accuracy in the estimates of the sensitivity measure, and (c) the computational cost involved. Next, the obtained results for both sensitivity analyses are discussed.

4.1.1.1. Local sensitivity analysis. The local sensitivity method computes the local gradients of the objective function (total annualized cost), in regard to infinitesimal parameter variation (P_j). Specifically, the analysis is focused on the relative marginal values (RMV_j) for each one of the model parameters which is defined as follows:

$$RMV_j = \frac{\frac{\partial(OF)}{OF}}{\frac{\partial(P_j)}{P_j}} = \frac{P_j}{OF} PMC_j \qquad \forall_j \tag{27}$$

where PMC_j refers to the parameter marginal cost and is computed as: $\frac{\partial(OF)}{\partial(P_j)}$.

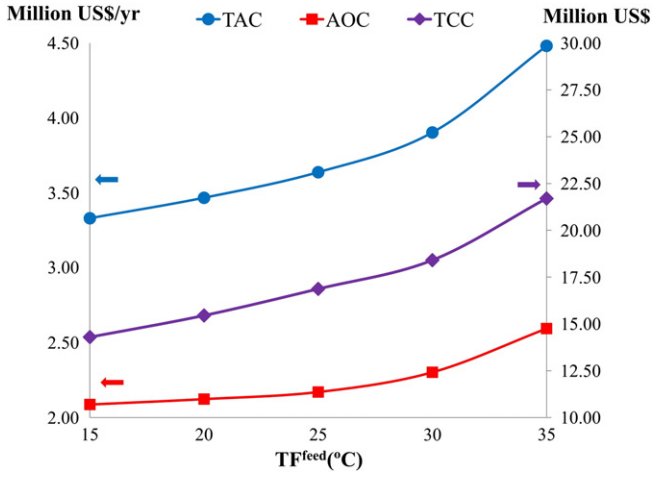

Fig. 10. TAC, AOC and TCC vs TF^{feed}.

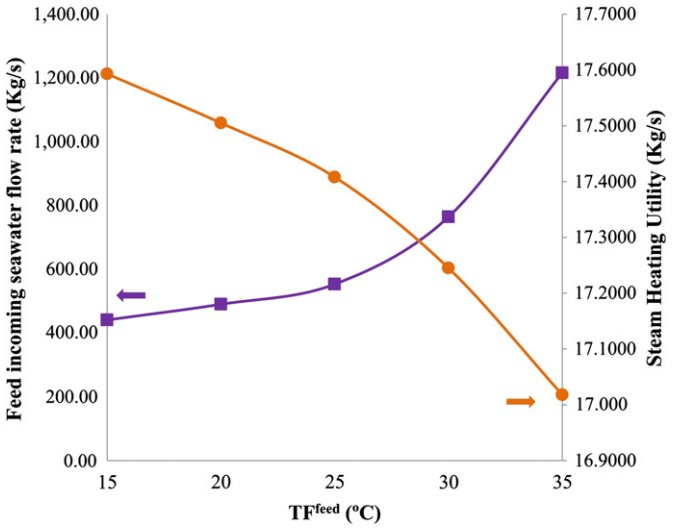

Fig. 11. F^{feed} and S vs TF^{feed}.

The direction of the change on the objective function is given by the sign of the RMV. As it is here defined, a positive relative marginal implies an increase in the specific total annualized cost when increasing the parameter value in 1%. Table 4 reports the values of RMV obtained for the main process parameters and they are arranged in order of importance, from the highest to the lowest effect on the total annualized cost.

For a more complete discussion, Figs. 4 to 7 compare the parameters per category. It can be easily observed that the seawater condition and the design parameters that have the maximal influences on the TAC are respectively TF^{feed} and TS, U^e and D. On the other hand, λ and BPE are the physical-chemical parameters with greater impact on the TAC. Finally, the most influential cost parameters are K^{MEE} and Cstm. At first glance, the results show that correlations instead of fixed values should be used to compute some physiochemical (λ, BPE, ρ^b and Cp^b) and design parameters (U^e) because they have strong influences on the model prediction. However, it is important to notice that the rank list previously presented in Table 4 is only useful to know which are the most sensitivity parameters in the "neighborhood" of the current optimal solution, but it does not identify which parameters must receive special attention in a wider range of variation. In order to get a more complete picture about the influence of each parameter, a more in-depth analysis is required, which is presented in the next section.

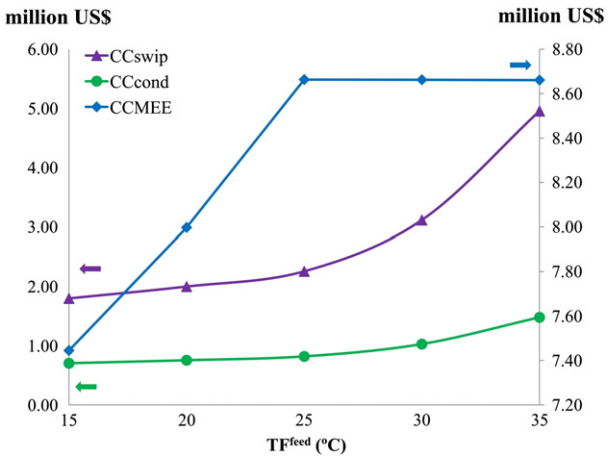

Fig. 12. Operating costs vs TF^{feed}.

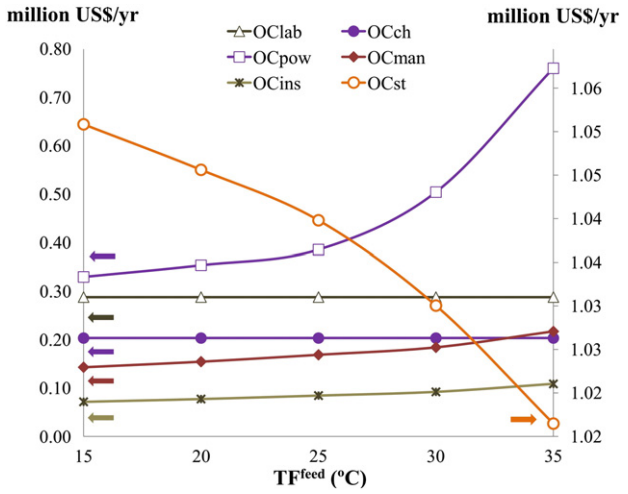

Fig. 13. Capital costs vs TF^{feed}.

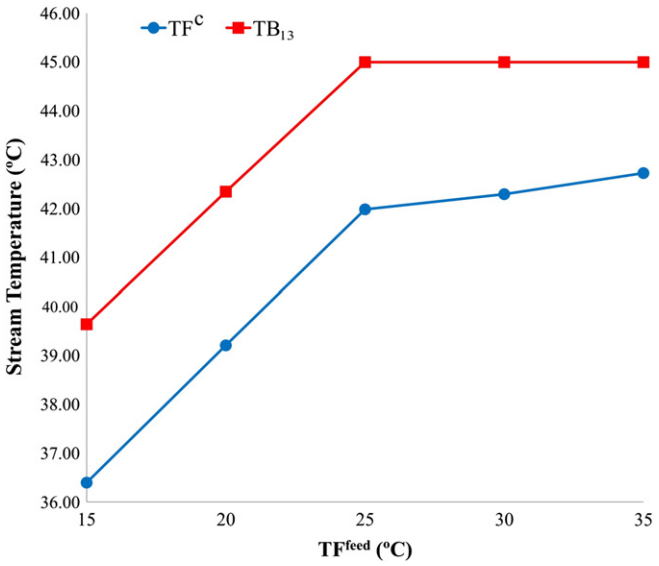

Fig. 15. TB_N and TFc vs TF^{feed}.

4.1.1.2. Global sensitivity analysis on the total cost. In order to perform the global sensitivity analysis, the parameter P_j, is varied around the nominal value listed in Table 1 while the remaining parameters are kept constant.

In this section, the discussion of result is divided into two parts. The former discusses the parameters that affect the TAC non-linearly and the second part analyses the parameters for which the TAC vary linearly.

4.1.1.2.1. Parameters with a nonlinear influence on the total annual cost
4.1.1.2.1.1. Influence of XB^{up} and T^{up} on the optimal design. From an environmental impact point of view, the maximum value of the reject stream salinity (XB_N) ranges from 60,000 to 80,000 ppm, and its temperature (TB_N) ranges from 25 to 50 °C, depending on the seawater conditions. From a theoretical point of view, the sensitivity analysis for XB^{up} and T^{up}, which are the upper bounds of XB_N and TB_N, is performed up to 150,000 ppm and 55 °C, respectively. Figs. 8 and 9 clearly show that the TAC decreases exponentially (around a 12%) with the increase of XB^{up} and T^{up}.

From the global material balance and since D cannot vary, as XB^{up} increases the flow-rates on preheaters (F) decreases. Thus, F^{feed} and S also decrease and thereby OCpow, CCswip, OCch and OCst. In addition, with the decrease of F and F^{feed}, the heat transfer area of the preheaters (A_j^p) and down condenser (A^c) and V_j^c also decrease, but D_j^e and the heat transfer area required by the evaporation effects (A_j^e) increases resulting in higher cost of the MEE unit (CCMEE) and therefore in higher TCC.

In regards to the T^{up} it was observed that despite the cost of heat transfer area required by the evaporation effects (CCMEE) and the cost of the heating utility (OCst) increase as T^{up} increases up to 45 °C, the cost of OCch, CCswip and CCcond decrease more significantly resulting in a lower total investment and operating costs. Certainly, results not presented here, show that the reason of the increase of CCMEE is that the driving force for the evaporation (ΔT, and then ΔT_j) decreases as T^{up} increases up to 45 °C, which results in higher heat transfer area. Results also show that the increase of T^{up} up to 45 °C leads to decrease the energy recovery from the brine stream, which results in higher requirement of heating utility (S) and OCst. On the other hand, CCcond decreases with the increasing of T^{up} as a consequence of the increase of the driving force for the condensation (which depends of TB_N and TF^{feed}). As expected, the cost of OCch and CCswip decrease with the decrease of the incoming seawater (F^{feed}). For higher values of T^{up} than 45.0 °C, the TAC does not vary because TB_N reached its optimal value (44.5 °C).

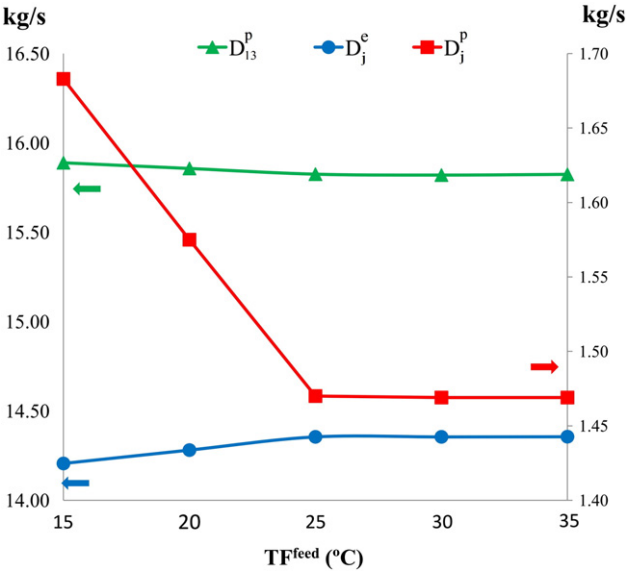

Fig. 14. Distilled vs TF^{feed}.

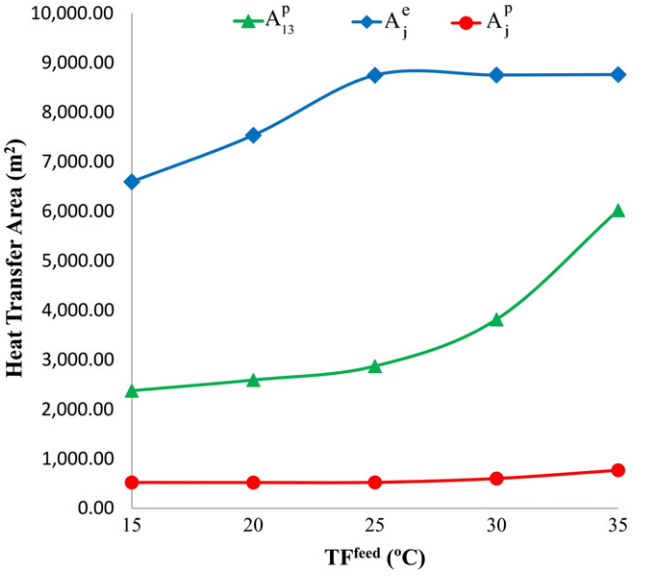

Fig. 16. Heat transfer areas vs TF^{feed}.

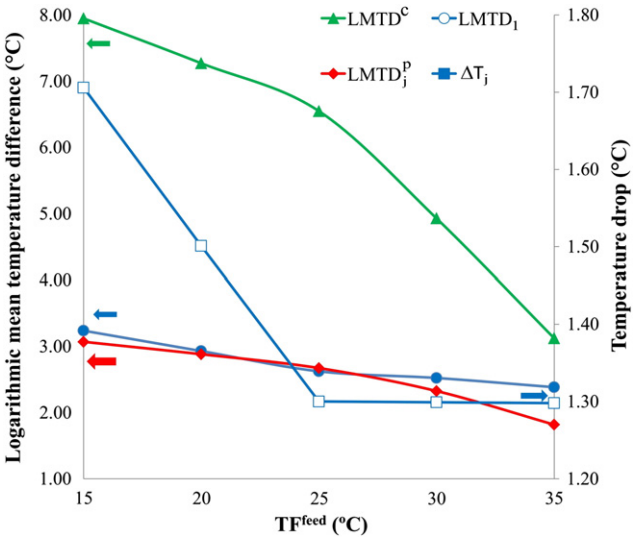

Fig. 17. ΔT and LMTD vs TF^{feed}.

4.1.1.2.1.2. Influence of TF^{feed} on the optimal design. Fig. 10 shows that the TAC significantly increases as TF^{feed} increases, following an exponential growth. For $TF^{feed} = 15.0$ and 35.0 °C the difference on the value of the TAC is about 35.0%.

The main reason of this increase can be explained as follows. Taking into account that both D and N are fixed, the distillate stream D_N^c remains almost constant, as shown in Fig. 14. Then, from the energy balance described in Eq. (28), the seawater flow-rate (F^{feed}) should increases as TF^{feed} increases, which leads to increase the seawater intake and pre-treatment capital cost (CCswip). In addition, considering Eq. (29), the increases of TF^{feed} leads to decrease the logarithmic mean temperature difference ($LMTD^c$) resulting in higher heat transfer A^c and thereby in higher investment cost (CCcond). Fig. 12 shows that the influence of CCswip on the total cost is higher than CCcond.

$$D_N^P \lambda = F^{feed} CP^b \left(TF^c - TF^{feed}\right) \tag{28}$$

$$A^c = \frac{F^{feed} CP^b \left(TF^c - TF^{feed}\right)}{U^c LMTD^c} \tag{29}$$

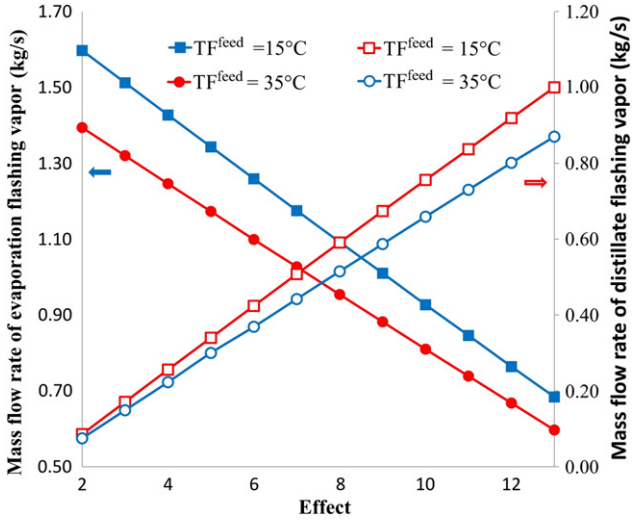

Fig. 18. V^{fd} and V^{fb} vs TF^{feed} and N.

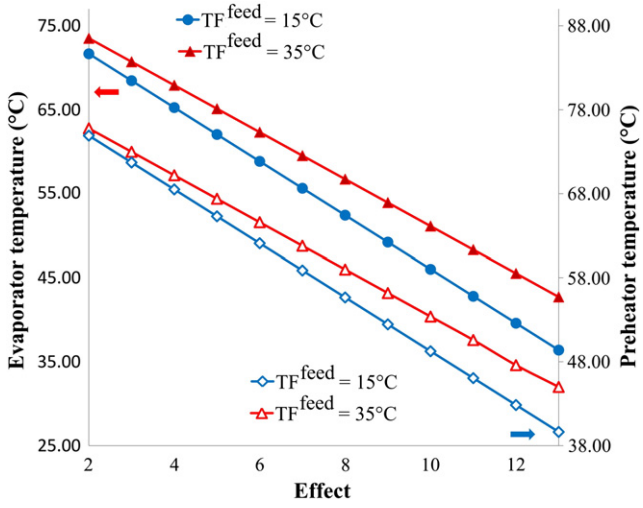

Fig. 19. T and TF vs number of effect and TF^{feed}.

By a similar reasoning, it is possible to analyze the effect of TF^{feed} on the CCMEE, which depends on the total heat transfer area used for evaporation (A_j^e). The temperature of distillate leaving the down-condenser (TB_N) increases as TF^{feed} increases resulting in a lower driving force in each evaporation effect (ΔT_j). Because D_j^e remains almost constant, Eq. (30) reveals that A_j^e increases with the increase of TF^{feed} resulting in higher investment cost (CCMEE).

$$D_j^e \lambda = A_j^e U^e \Delta T_j = A_j^e U^e \left(TV_j^b - TB_j\right) \tag{30}$$

It is interesting to observe the behavior of CCMEE in Fig. 12 when TF^{feed} is higher than 25 °C. As was already said, the increase of TF^{feed} leads to increase TB_N and TF^c (seawater temperature leaving the down-condenser). However, TB_N reaches its upper bounds (T^{up}) from $TF^{feed} = 25$ °C as shown in Fig. 15. This is the main reason of why CCMEE, D_j^c, D_j^e, A_j^e and ΔT_j do not vary from $TF^{feed} = 25$ °C. (See Figs. 16 and 17).

On the other hand, it is widely known that as the total heat transfer area increase, the steam consumption (S) decrease. In agreement with this, Figs. 11 and 13 show that the steam consumption (S) and thereby its cost (OCst) slightly decrease with the increasing of TF^{feed}. However, as the increase of OCpow is more significant than the decrease of OCst, AOC increases (Fig. 10).

Finally, the flow-rates of vapor formed by the brine flashing in each evaporation effect (V_j^{fb}) and by distillate flashing (V_j^{fd}) vary with TF^{feed} along the unit and they are illustrated in Fig. 18. As shown, V_j^{fb} decreases

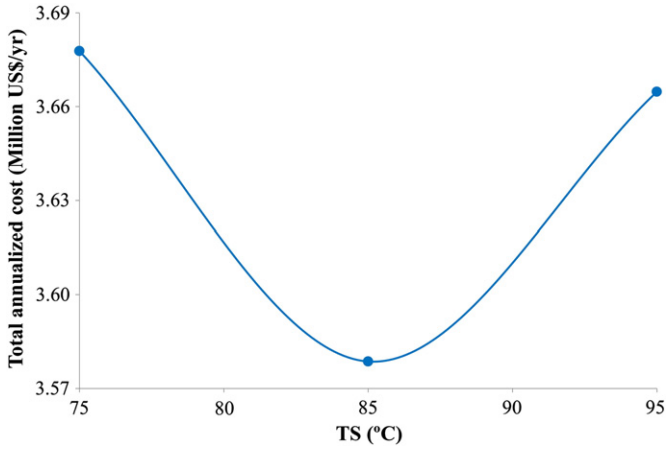

Fig. 20. Total annualized costs vs TS.

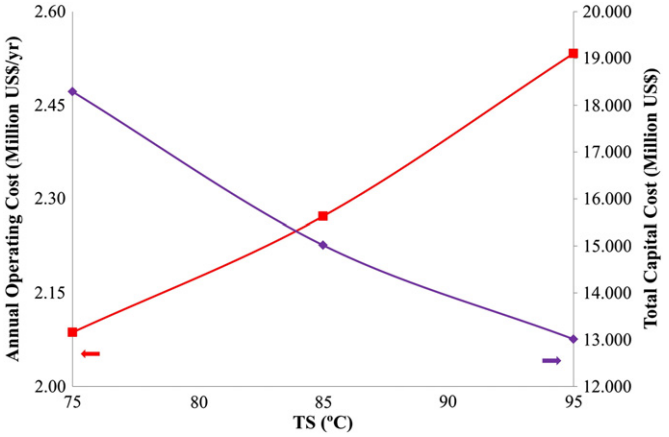

Fig. 21. Operating and capital costs vs TS.

linearly from the second to the last effect as TF^{feed} increases whereas V_j^{fd} increases. Note that the sum of V_j^{fb} and V_j^{fd} from the second effect is equal to D_j^c, and then, the flow-rates of distillate leaving the pre-heaters (D_j^c) and evaporation effects (D_j^e) remains constants in all effects (Fig. 14). Fig. 19 shows the profiles of T_j and TF_j^p along the MEE unit for different values of T^{Feed}.

4.1.1.2.1.3. Influence of TS on the optimal design. Fig. 20 shows the variation of the TAC with TS. As shown, the lowest value of TAC is 3.6 million US$/yr and it is reached at TS = 85 °C. It is also observed that by increasing TS from 75 to 85 °C, the TAC decreases around a 3% (3.7 to 3.6 million US$/yr). Figs. 21 to 23 show how TS affects the investment and operating total cost and how these costs are distributed. As expected, the capital cost decreases as TS increases because of a significant decrease in CCMEE (Figs. 21 and 23) whereas the total operating cost increases with the increasing of TS because of a significant increase in OCst (Fig. 22).

For a complete presentation of results, Figs. 24 to 29 show how the different trade-offs vary with TS. As shown in Fig. 24, the increase of TS leads to increase $LMTD_1$ and the temperature drop for evaporation (ΔT_j) resulting in a reduction of the corresponding heat transfer areas (A_j^e) and therefore V_j^b. From an energy balance on down condenser, it is possible to conclude that while TS increases F^{feed} decreases. Actually, Fig. 26 shows that as TS increases from 75 to 85 °C, F^{feed} decreases by 15% (from 617 kg/s to 525 kg/s) and then it remains almost constant. On the other hand, as the total heat transfer area is reduced a 50%

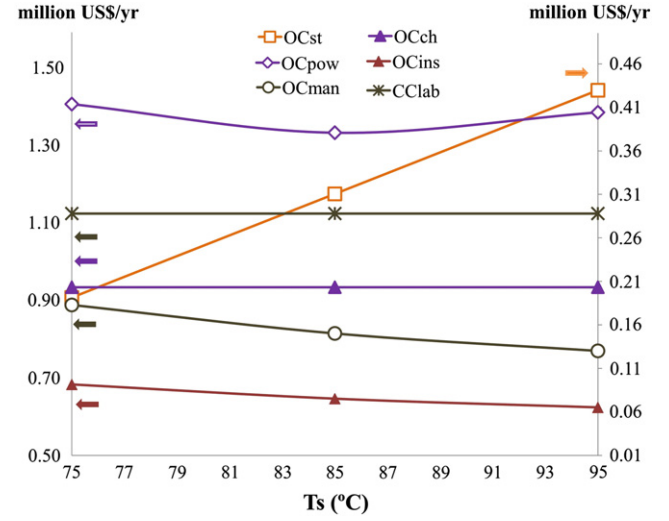

Fig. 22. Operating costs vs TS.

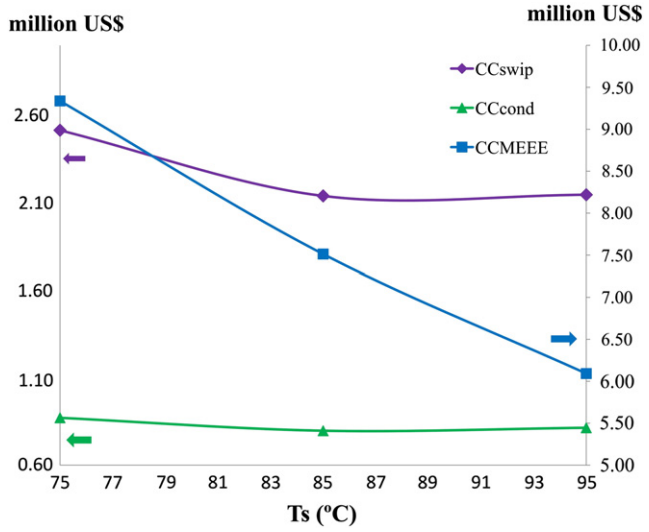

Fig. 23. Capital costs vs TS.

(140,745.028 m^2 to 70,032.837 m^2) the steam consumption S increases by 1% (17.35 kg/s to 17.55 kg/s) from TS = 75 to 95 °C.

As the total distillate is given and V_j^b decreases, V_j^c increases. Then, from an energy balance on the pre-heater, it is possible to conclude that while V_j^c increases, TF_j^c and the logarithmic mean temperature difference ($LMTD_j^c$) and the heat transfer area of pre-heaters (A_j^c) increase with the increase of Ts (Figs. 24 and 25). Finally, Fig. 29 shows the distribution of V_j^{fb} and V_j^{fd} along the MEE unit.

4.1.1.2.1.4. Influence of N on the optimal design. At this point, it is important to mention that the proposed model was implemented in such a way that each effect is modeled by using an index ("j") which varies from 1 to J. Then, to run the model, the user fixes the number of effect by assigning a value for J. This is why the local sensitivity analysis cannot be applied for N and the influence of N on TAC was not discussed previously. In this section, a global sensitivity analysis of N varying the index J is discussed.

Fig. 30 shows that the TAC is strongly influenced by N. A minimum value of TAC equal to 3.58 million US$ is reached at N = 12. As can be seen, this is the result of the existing trade-off between the operating annual cost (AOC) and the investment cost (TCC), while AOC decreases

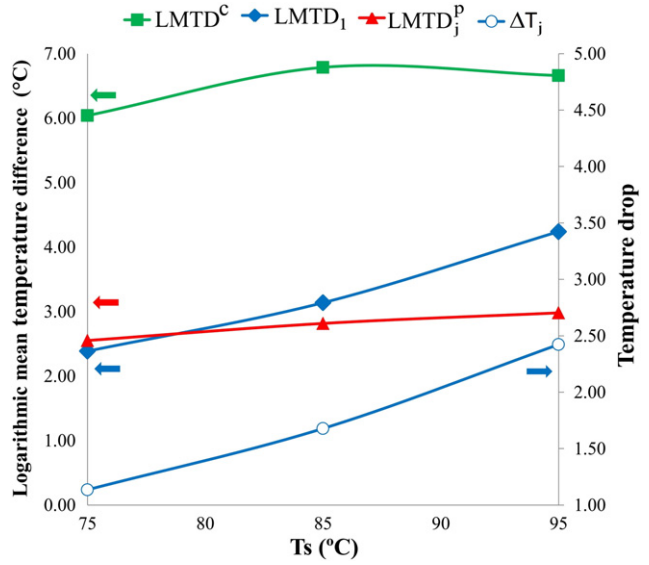

Fig. 24. ΔT and LMTD vs TS.

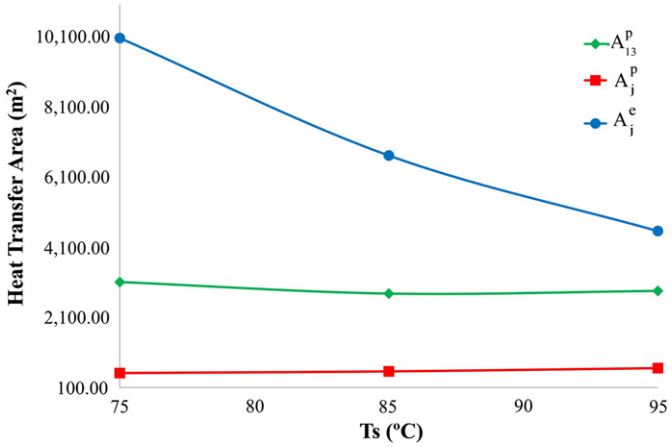

Fig. 25. Heat transfer areas vs TS.

in a continuous way with the increasing of N, TCC decreases until N = 8 and then it increases significantly. The decrease of AOC is mainly caused by the decrease of the cost of the heating utility consumption (OCst), whereas the increment of TCC is mainly caused by the increase of CCMEE. The behavior of these costs can be explained as follows.

According to Eq. (31) and considering that the total distillate produced on the system (D) is fixed, it is possible to conclude that D^e_j decreases as N increases.

$$D^e_j = \frac{D}{N} - \frac{\sum_{J=2}^{N} D^{fb}_j}{N} \tag{31}$$

On the other hand, because $TV^b_{1\ and}$ TB_N are free variables (they are not fixed), ΔT_j may vary not only by N but also by ΔT. Certainly, the results obtained shown that ΔT increases as N increases. However, the rate of increment of N is higher than the rate of increment of ΔT, and then by Eqs. ((32) and (33)), ΔT_j decreases.

$$\Delta T = TS - TB_N + \sum_{j=1}^{N} BPE \tag{32}$$

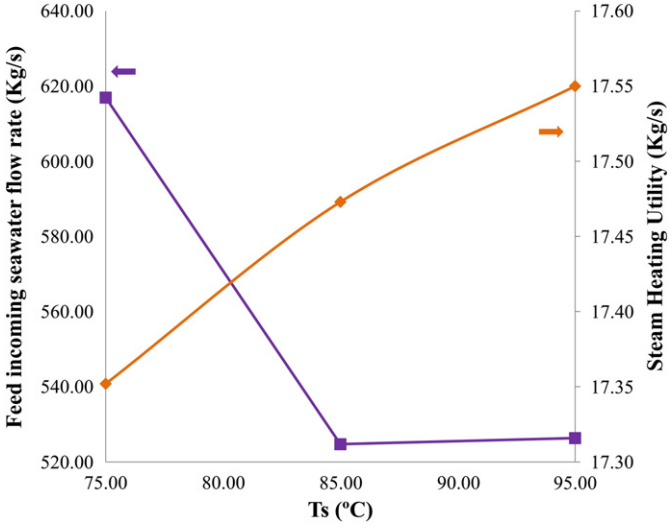

Fig. 26. F^{feed} and S vs TS.

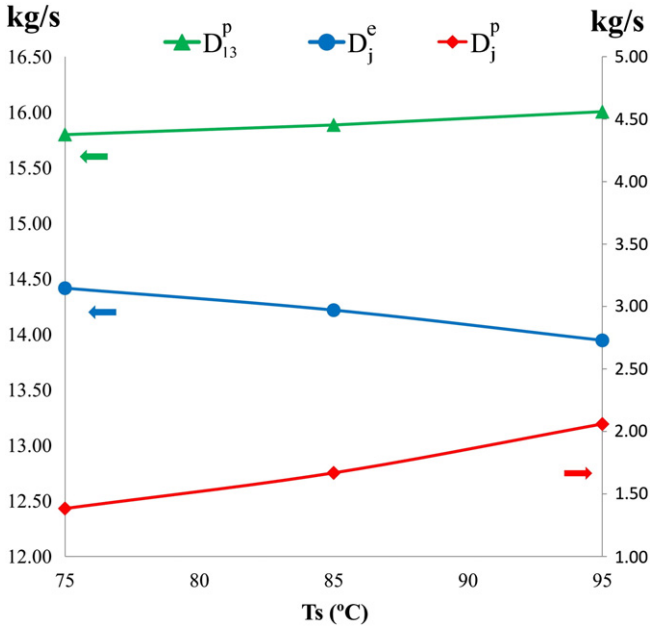

Fig. 27. Distilled vs TS.

$$\begin{cases} \Delta T_j = TS - TB_1 & J = 1 \\ \Delta T_j = \dfrac{\Delta T^m}{N} = \dfrac{\left(TV^b_1 - TB_N + \sum_{j=2}^{N} BPE\right)}{N} & J = 2-N \end{cases} \tag{33}$$

Observing Eq. (34) it is possible to see that if D^e_j and ΔT_j decrease, A^e_j must be modified in order to maintain the balance. According to the obtained results A^e_j decreases until N = 6, but after that it increases rapidly until N = 12, where there is a new inflection point and the rising rate decreases.

$$A^e_j = \frac{D^e_j \lambda}{U \Delta T_j} \tag{34}$$

According to Eqs. (10) and (11), CCMEE is a function of A^{MEE} (total effects evaporation transfer area), which in turn depends on N and A^e_j. Despite the variation of A^e_j, A^{MEE}, and thereby CCMEE, increases as N increases because the rate of increment of N.

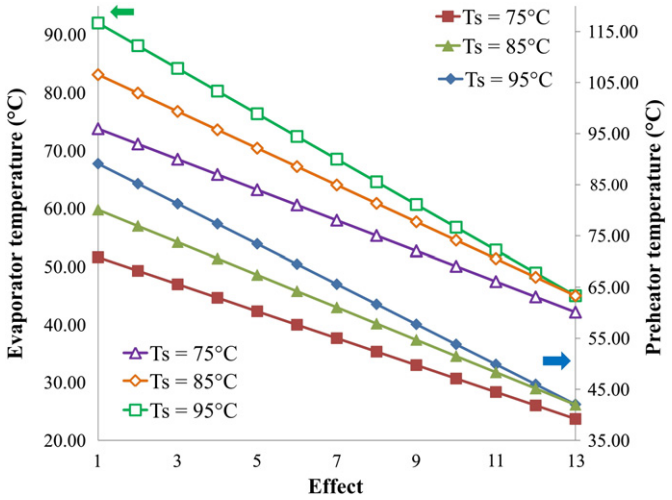

Fig. 28. T and TF vs number of effect and TS.

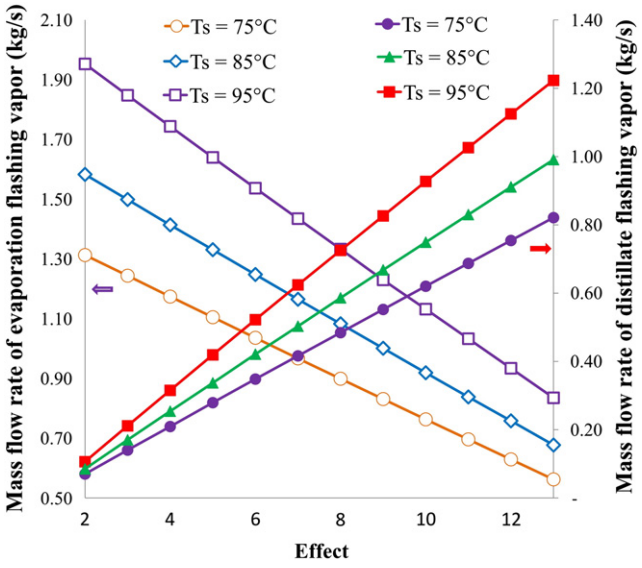

Fig. 29. V^{fd} and V^{fb} vs TS and N.

As is widely known, the higher the total heat transfer area the lower the steam consumption (S) and thereby the lower the heating utility cost (OCst). For instance, S decreases by 72% (52 kg/s vs. 14 kg/s) and A^{MEE} increases by 530% (22.312 m^2 vs. 140.484 m^2) for N = 4 to N = 16, respectively. For N = 4 and 12 the difference on the value of the TAC is about 41.0%.

4.1.1.2.2. Parameters with a linear influence on the total annual cost. From the obtained results not presented here, it is also possible to conclude that the

TAC is linearly affected by the remaining model parameters listed in Table 4.

Thus, information obtained by the local sensitivity method presented above for these parameters can be used.

Of all parameters related to the physical–chemical properties, the most relevant parameter resulted to be the BPE. For instance, considering that the BPE depends on the temperature and salinity, it may vary from 1.0 to 2.0 °C (100%) affecting the objective function around a 22.0%. On the other hand, λ may vary from 2256.0 to 2412.0 kJ/kg (7.0%) and Cp^b from 4.0 to 4.8 kJ/kg (20.0%). Then, according to their RVM values, they may affect the objective function around a 7.0 and 2.0% respectively.

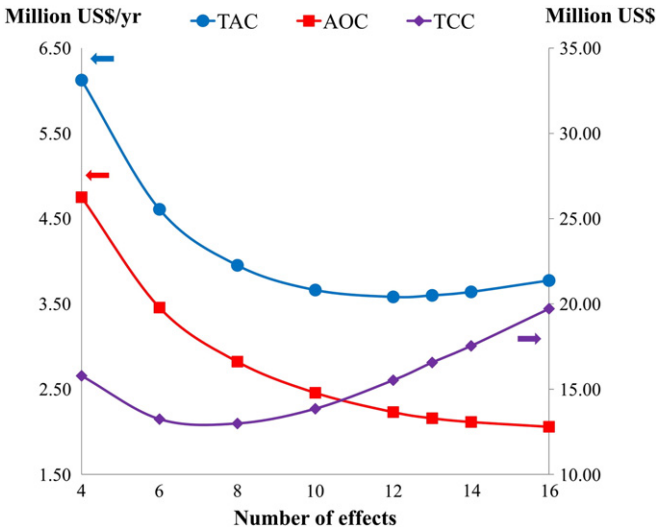

Fig. 30. TAC, AOC and TCC vs N.

Table 5
List of the most influential parameters for the minimization of TAC.

Parameters	Percentages
Number of stage (N)	41.0%
Seawater temperature (TF^{Feed})	35.0%
Steam temperature used as heating utility (TS)	25.0%
Boiling point elevation (BPE)	22.0%
Overall heat transfer coefficient in evaporator (U^e)	19.0%
Rejected brine temperature (T^{UP})	11.4%
Rejected brine salinity (X^{UP})	10.0%

With regard to the design parameters, D and U^e have strong influences on the TAC. As expected, the TAC increases with the increase of D. The parameter U^e may vary from 2.0 to 4.0 kW/(m^2 °C) (100.0%) affecting the objective function around a 19.0%.

Finally, the TAC is also strongly influenced by K^{MEE} and Cstm. For this reason, up-date values on these parameters are essential for the design of new desalting plants.

Up to this point, it is possible to conclude that the most influential parameters for the minimization of TAC are listed in Table 5.

From a mathematical modeling point of view, the results showed in Table 5 reveal that BPE and U^e should be computed using correlations instead of use known and fixed values. From a practical application point of view, special attention should be put on the following operating conditions when the TAC is analyzed: TF^{feed}, TS, T^{up} and X^{up}. The following special comment needs to be made for TF^{feed} (feed stream), XB^{up} and T^{up} (reject stream) if hybrid desalination systems are proposed. Thus, the incoming seawater may be thermally integrated with other stream(s) of other process(es). In addition, the rejected brine stream may be also integrated with other stream(s) through its temperature and salinity.

4.2. Case study 2: maximization of the fresh water production for a nominal design

4.2.1. Sensitivity analysis of the model parameters on the distillate production

Finally, the resulting model was also used to identify the operating conditions that should be modified, for the same optimal size of the MEE unit obtained in Section 4.1 (Table 2), in order to increase the fresh water over the nominal capacity of production. To do this, the model was used in simulation mode and solved by fixing the heat transfer areas (evaporation effect and pre-heaters) and feed seawater flow

Table 6
Local sensitivity analysis — Relative marginal values (RMV).

Parameters		Value	RMV
F^{feed}	(kg/s)	540.00	4.14
T^s	(°C)	80.00	2.14
λ	(kJ/kg)	2375.00	−0.97
TF^{feed}	(°C)	24.00	−0.64
BPE	(°C)	1.50	−0.53
U^e	(kW/m^2 °C)	3.00	0.47
Cp^b	(kJ/kg °C)	4.00	0.42
A^e_{12}	(m^2)	8484.66	0.08
U^p	(kW/m^2 °C)	2.50	0.04
$A^e_{j=4,5}$	(m^2)	8484.66	0.04
A^e_1	(m^2)	9133.279	0.04
A^p_3	(m^2)	521.09	−0.04
A^e_6	(m^2)	8484.66	0.04
U^c	(kW/m^2 °C)	2.00	0.04
A^p_{12}	(m^2)	521.09	0.04
$A^e_{j=7-11,13}$	(m^2)	8484.66	0.03
A^p_4	(m^2)	521.09	0.03
A^e_2	(m^2)	8484.66	0.03
A^p_5	(m^2)	521.09	0.01
A^p_2	(m^2)	521.09	−0.01
A^p_6	(m^2)	521.09	0.01

Table 7
Optimal values for the main variables of the system (fresh water production = 240 kg/s).

Variables		Value	Percent
F^{feed}	(kg/s)	663.00	23%
Ts	(°C)	83.77	5%
F	(kg/s)	340.00	28%
S	(kg/s)	22.00	25%
F^{c}	(kg/s)	264.00	16%
T_1	(°C)	80.50	4%
TF^{c}	(°C)	41.00	−1%
sAOC	(US$/m^3)	0.395	5%
AOC	(million US$/yr)	2.73	26%
OCst		1.42	36%
OCpow		0.44	17%
OClab		0.35	20%
OCch		0.26	28%
OCman		0.17	4%
OCins		0.09	4%

rate listed in Table 2 but using another objective function: Certainly, the fresh water production (maximization) is the new objective function instead of the total annual cost (minimization).

As expected, the solution for this case is the same to that obtained in the previous case, because there are no degrees of freedom. However, the marginal contribution of each parameter to the new objective function is different. Table 6 reports the values of RMV of the parameters that have a significant influence on the fresh water production. Here, it is important to explain that the heat transfer areas and the incoming seawater flow rate are considered as model parameters, in contrast to the previous case of optimization. For this reason, they are included in Table 6.

The results of a comparison between Tables 4 and 6 clearly reveal the following findings:

a) As expected, the values of the parameter's RMV have changed and therefore the rank list has been altered.
b) Cp, TF^{feed}, TS, U^{e}, U^{p}, U^{c}, λ and BPE have strong influence on the maximization of D than on the minimization of TAC.
c) THY, K^{MEE}, K^{C}, Cstm, XF^{feed}, XB^{up}, Cpow, η, Cswip, Clab, Cch, ΔP^{in}, ρ^{p}, ρ^{b}, dca, dci and ν^{b} are more sensitive to the total annual cost than on the fresh water production.
d) The seawater flow rate (F^{Feed}) and the steam temperature (TS) are the only operating parameters that may be modified in order to improve significantly the distillate production when the nominal design is fixed. The higher values of F^{feed} and TS the higher values of D.

Then, the model was solved to determine the optimal solution in order to increase the fresh water production in 20.0% over the nominal capacity of production (200.0 kg/s). In contrast to the optimization problem discussed in Section 4.1, the seawater flow rate and the steam temperature are now considered as optimization variables. However, the same nominal design discussed in Section 4.1 is assumed. Therefore, the total annual operating cost is the new objective function to be minimized because the total investment is invariant. Table 7 lists the obtained optimal values and the distribution of the total operating cost. In addition, the third column of Table 7 shows the percent of variation of each variable compared to that obtained in Section 4.1. Fig. 31 shows the flow-rate, temperature and salinity for each stream per effect.

As shown in Table 6, the highest increase is observed for the cost related to the heating utility (OCst) which increased in about 36% whereas the OCpow, OClab and OCch increased, respectively, 17.0, 20.0 and 28.0%. It is important to notice that the increase of the incoming seawater flow rate (F^{feed}) may require an additional seawater pump which can be operated in parallel model.

5. Conclusion

A previous mathematical model developed recently by the authors was extended to determine cost-effective designs of the MEE desalination system. Given the seawater conditions, the proposed mathematical model was solved for the following two case studies.

a) To determine the optimal sizing of equipment and optimal operation conditions that satisfies a fixed nominal production of fresh water at minimum total annual cost.

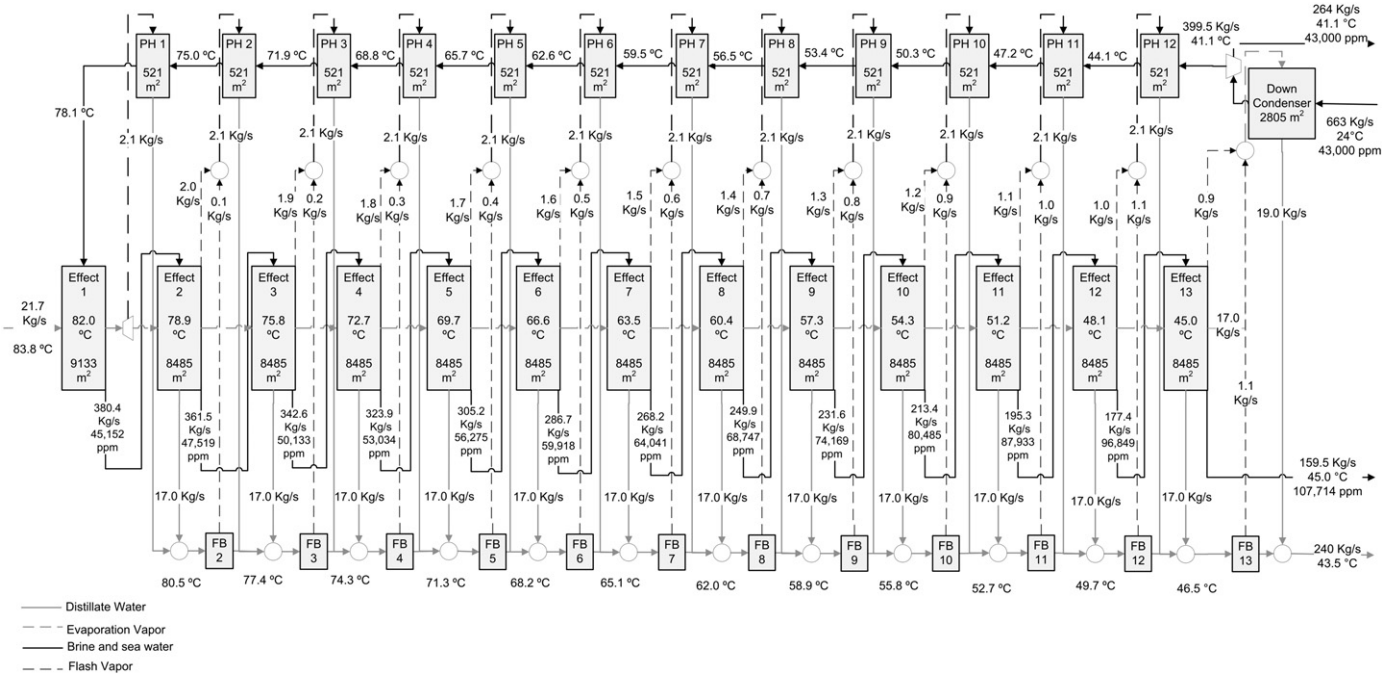

Fig. 31. Optimal Solution for a fresh water production of 240 kg/s.

b) To investigate the possibility to increase the distillate production over the nominal capacity considered in a) but using the same nominal design.

From the optimization results and sensitivity analyses particular conclusions are obtained which can be applied in practical way for new and existing MEE units. In addition, valuable guidelines to be considered for the development of rigorous and more realistic mathematical models are identified.

From a practical point of view, the possibility to increase the distillate production over the nominal capacity of an existing MEE unit was studied. The obtained results indicate that the seawater flow rate and the steam temperature are the only operating parameters that should be modified. For instance, for an existing MEE unit with 120,000.0 m^2 of total heat transfer area, the seawater flow rate and steam temperature must increase by 23.0 and 5.0%, respectively (540.0 vs. 663.0 kg/s and 80.0 vs. 83.7 °C) to increase the distillate production by 20.0% over the nominal capacity (200.0 kg/s). It is important to notice that the increase of the incoming seawater flow rate (F^{feed}) may require an additional seawater pump which can be operated in parallel mode.

From a mathematical modeling aspect, the sensitivity analysis indicates that BPE and U^e should be computed using correlations instead of use known and fixed values, because they have strong influence on the model prediction. From a practical application point of view, special attention should also be put on the following operating conditions when the TAC is analyzed: TF^{feed}, TS, T^{up} and X^{up}. A special comment needs to be made for TF^{feed}, XB^{up} and T^{up} if hybrid desalination systems are proposed. Certainly, the incoming seawater and the rejected brine stream may be efficiently integrated with other stream(s) of other process(es).

Currently, the presented model is being extended in order to consider the number of effects as an optimization variable (discrete decision). The inclusion of the geometry (height, length and width) and pressure drop are also being considered. In addition, the dependence of the boiling point elevation, non-equilibrium allowance and the global heat transfer coefficient will also be included. These inclusions require the introduction of new variables such as: velocity on the inside of the tube, tube size and pitch arrangement.

Finally, the coupling of the MEE system and SOFT cells (Solid Oxide Fuel Cell) and RO system will be further investigated in detail.

Nomenclature

A	heat transfer surface area, m^2
B	brine flow rate, kg/s
BPE	boiling point elevation, °C
BRINE	total brine flow rate rejected from the hybrid system, kg/s
CP^b	specific heat at constant pressure of brine, kJ/kg °C
CR	conversion Ratio, kg/s of D/(kg/s of F)
D	mass flow rate of distillate, kg/s
F	feed flow rate, kg/s
Feed	total feed flow from the sea rate to de hybrid system, kg/s
H	water enthalpy, kJ/kg
LMTD	logarithmic mean temperature difference, °C
N	total number of effects
NEA	non-equilibrium allowance, °C
P	saturation pressure, bar
PR	performance Ratio, kg/s of D/(kg/s of S)
S	heating steam, kg/s
sA	specific total heat transfer area, m^2/(kg/s of D)
sWc	specific cooling water rate, kg of F^c/s/(kg/s of D)
sQ	specific total heat, kJ/s/(kg/s of D)
T	stream temperature, °C
U	overall heat transfer coefficients, kW/(m^2 °C)
Q	heat flux, kJ/s
V	mass flow rate of vapor, kg/s
X	salt concentration, ppm
W	electric energy

7. Cost model

CRF	capital recovery factor
sAOC	specific annual operating cost, US$/yr
AOC	annual operating cost, US$/yr
Carea	area cost parameter, US$/$m^2$
CCcw	civil work capital cost, US$
CCeq	total equipment capital cost, US$
CCswip	seawater intake and pre-treatment capital cost, US$
CCMEE	MEE capital cost, US$
CCcond	down condenser capital cost, US$
CCDir	direct capital cost, US$
CCIndr	indirect capital cost, US$
Cch	chemical treatment cost, $/$m^3$
Clab	labor cost factor, US$/$m^3$
Cmat	material correction factor
Cpow	electricity cost, US$/kWh
Cstm	steam cost, US$/kg
Cswip	seawater intake and pre-treatment cost for MEE, US$/($m^3$/d)
Dca	tube external diameter, m
Dci	tube internal diameter, m
Ir	expected annual interest rate
K	cost co-factor, US$/$m^2$
KCch	chemical treatment cost, US$/$m^3$
KClab	labor cost factor, US$/(yr kg/s)
KCswip	seawater intake and pre-treatment cost for MEE, US$/(yr kg/s)
KCpow	electricity cost, (US$ Pa m^3/kWyr bar kg)
KCstm	steam cost, US$/(kg/s yr)
L	length, m
Nt	tubes number
OCch	chemical treatment operational cost, US$/yr
OClab	operation cost, US$/yr
OCins	steam operational cost, US$/yr
OCman	maintenance cost, US$/yr
OCpow	energy operational cost, US$/yr
OCst	steam operational cost, US$/yr
Scal	scaling exponent
sTAC	specific annualized cost of fresh water per kg/s, US$/kg/s
Re	Reynolds number
TAC	total annualized cost, US$/yr
TCC	total capital cost, US$
THY	annual operational time, h/yr
Time	lifetime of the plant
RHC	hydrodynamic resistance of the connection pieces
RHin	hydrodynamic resistance of the inlet
RHout	hydrodynamic resistance of the outlet
RHben	hydrodynamic resistance of a bend

8. Greeks

ε	void fraction
λ	latent heat, kJ/kg
ρ	average density (kg/m^3)
ν	viscosity (kg/m s)
η	efficiency
ΔT	temperature drop
ΔP^{in}	Pressure drop in the intake system

9. Superscript

b	vapor formed by boiling
be	vapor formed by boiling directed to the next evaporator
c	cooling seawater
e	evaporator
f	feed flow rate in preheaters
fb	vapor formed by flashing inside the effects

fd	vapor formed by flashing inside the flashing boxes
feed	total feed seawater
fin	flow in the flashing box
fot	flow out the flashing box
p	preheater
up	upper bound, ppm

10. Subscripts

i: 1,2,...n effect number

Acknowledgment

The authors would like to acknowledge financial support received from Consejo Nacional de Investigaciones Científicas y Tecnológicas (CONICET) and Agencia Nacional de Promoción Científica y Tecnológica (ANPCYT) Argentina.

Appendix A. Complementary equations

$$\text{acf} = \frac{(\text{ir}+1)^{\text{THY}}\text{ir}}{(\text{ir}+1)^{\text{THY}}-1} \tag{A.1}$$

$$\Delta P^{c} = \left(\text{RHC} + \text{RHin} + \frac{0.3164 L_c}{\text{Re}_c^{0.25} d_{ci}} + \text{RHout} + \text{RHC} + 3\text{RHben}\right) U_c^2 \frac{\rho}{2} 10^{-5} \tag{A.2}$$

$$L_i^c = \frac{A^c}{\Pi\ \text{dca}\ \text{nt}_c} \tag{A.3}$$

$$\text{nt}_c = \frac{4\ F^{\text{feed}}}{\Pi\ \rho\ U^c\ \text{dci}^2} \tag{A.4}$$

$$\text{Re}_c = \frac{\rho^b\, U^c\, \text{dci}}{\nu^b} \tag{A.5}$$

$$\Delta P^{p} = (N-1) \times \left(\text{RHC} + \text{RHin} + \frac{0.3164 L_p}{\text{Re}_p^{0.25} d_{ci}} + \text{RHout} + \text{RHC} + \text{RHben}\right) U_p^2 \frac{\rho}{2} 10^{-5} \tag{A.6}$$

$$L_i^p = \frac{A_i^p}{\Pi\ \text{dca}\ \text{nt}_c} \tag{A.7}$$

$$\text{nt}_p = \frac{4\ F}{\Pi\ \rho\ U^c\ \text{dci}^2} \tag{A.8}$$

$$\text{Re}_p = \frac{\rho^b\, U^p\, \text{dci}}{\nu^b} \tag{A.9}$$

$$\Delta P^{e} = P_1\left(TD_{_1}\right) \text{-} P_N(TD_N) \tag{A.10}$$

$$\left(\ln\left(\frac{P_i}{10}\right)-9.49\right)\ (T_i + 237.15) = \left(\ln\left(\frac{P_i}{10}\right)-9.49\right)\ 42.7\text{-}3892 \tag{A.11}$$

References

[1] D.K. Akili, K.K. Ibrahim, W. Jong-Mihn, Advances in seawater desalination technologies, Desalination 221 (2008) 47–69.
[2] M.A. Darwish, F. Al-Juwayhel, H.K. Abdulraheim, Multi-effect boiling systems from an energy viewpoint, Desalination 194 (2006) 22–39.
[3] H.T. El-Dessouky, H.M. Ettouney, F. Mandani, Performance of parallel feed multiple effect evaporation system for seawater desalination, Appl. Therm. Eng. 20 (2000) 1679–1706.
[4] E. Cardona, A. Piacentino, Optimal design of cogeneration plants for seawater desalination, Desalination 166 (2004) 411–426.
[5] E. Cardona, A. Piacentino, Optimal advanced energetics of a multiple effects evaporation (MEE) desalination plant. Part I: 2nd principle analysis by a zooming representation at single-effect level, Desalination 264 (2010) 84–91.
[6] A.S. Nafey, H.E.S. Fath, A.A. Mabrouk, Thermoeconomic design of a multi-effect evaporation mechanical vapor compression (MEE–MVC) desalination process, Desalination 230 (2008) 1–15.
[7] A.A. Mabrouk, A.S. Nafey, H.E.S. Fath, Thermoeconomic analysis of some existing desalination processes, Desalination 205 (2007) 354–373.
[8] A.S. Nafey, H.E.S. Fath, A.A. Mabrouk, Thermo-economic investigation of multi effect evaporation (MEE) and hybrid multi effect evaporation–multi stage flash (MEE–MSF) systems, Desalination 201 (2006) 241–254.
[9] Y. Wang, N. Lior, Thermoeconomic analysis of a low-temperature multi-effect thermal desalination system coupled with an absorption heat pump, 54 (2011) 5497–5503.
[10] H. Sayyaadi, A. Saffari, Thermoeconomic optimization of multi effect distillation desalination systems, Appl. Energy 87 (4) (2010) 1122–1133.
[11] P.A. Aguirre, S.F. Mussati, P. Druetta, Optimization of multi-effect evaporation desalination plants, Desalination 311 (2013) 1–15.
[12] N.M. Wade, Distillation plant development and cost update, Desalination 136 (2001) 3–12.
[13] Desalting handbook for planners, Desalination and Water Purification Research and Development Program 72, United States Department of the Interior, Bureau of Reclamation, Water Treatment Engineering and Research Group, 2003.
[14] M. Skiborowski, A. Mhamdi, K. Kraemer, W. Marquardt, Model-based structural optimization of seawater desalination plants, Desalination 292 (2012) 30–44.
[15] F. Vince, F. Marechal, E. Aoustin, P. Breant, Multi-objective optimization of desalination plants, Desalination 222 (2008) 96–118.
[16] A.M. Helal, A.M. El-Nashar, E. Al-Katheeri, S. Al-Malek, Optimal design of hybrid RO/MSF desalination plants part I: modeling and algorithms, Desalination 154 (2003) 43–66.
[17] M.H. Khoshgoftar Manesh, H. Ghalami, M. Amidpour, M.H. Hamedi, Optimal coupling of site utility steam network with MED-RO desalination through total site analysis and exergoeconomic optimization, Desalination 316 (2013) 42–52.
[18] N. Ghaffour, T.M. Missimer, G.L. Amy, Technical review and evaluation of the economics of water desalination: current and future challenges for better water supply sustainability, Desalination 309 (2013) 197–207.
[19] M.A. Sharaf, A.S. Nafey, L. García-Rodríguez, Thermo-economic analysis of solar thermal power cycles assisted MED-VC (multi effect distillation-vapor compression) desalination processes, Energy 36 (2011) 2753–2764.
[20] I.C. Karagiannis, P.G. Soldatos, Water desalination cost literature: review and assessment, Desalination 223 (2008) 448–456